RELATIONSHIP BETWEEN THE DYNAMICS OF ELECTRON FLUXES IN THE EARTH'S OUTER RADIATION BELT AND THE DEVELOPMENT OF A RING CURRENT 17-18.03.2015 and 22-23.06.2015

© 2025 Azra-Gorskaya C. G.[a,b,] *, Zykina A. A.[a,b], Kalegaev V. V.[a,b], Vlasova N. A.[a], Nazarkov I. S.[a]

[a]*Skobeltsyn Research Institute of Nuclear Physics, Moscow State University, Moscow, Russia*

[b]*Moscow State University, Faculty of Physics, Moscow, Russia*

**e-mail: clemenceanastasia@gmail.com*

Received March 10, 2025

Revised April 12, 2025

Accepted May 22, 2025

Abstract. The article presents the results of studies of variations in the proton fluxes of the ring current and relativistic electrons of the Earth's outer radiation belt, as well as the magnetospheric magnetic field during two geomagnetic storms of March 17–18, 2015 and June 22–23, 2015 of similar power ($|Dst_{max}|$~200 nT), caused by different conditions in the solar wind. The work is based on experimental data from the Van Allen Probes spacecraft. The results of comparison of simultaneous measurements of proton and electron fluxes and the magnetospheric magnetic field during geomagnetic storms indicate a consistent dynamics of the ring current and the Earth's outer radiation belt. It is shown that variations in the magnetic field, occurring due to the development of the ring current and substorm activations, are the main factors responsible for the dynamics of the relativistic electron fluxes of the outer radiation belt during the geomagnetic storms of March 17-18, 2015 and June 22-23, 2015.

Keywords: *magnetosphere, magnetic storms, Earth's radiation belts, electron outer radiation belt, magnetospheric magnetic field*

DOI: 10.31857/S00167940250504e3

1. INTRODUCTION

The Earth's magnetosphere is under the constant and active influence of the interplanetary medium. The magnetosphere is formed by the magnetic fields of the planet and magnetospheric current systems. The interplanetary medium is inhomogeneous and nonstationary, and the

magnetosphere is a self-organizing system, so the response of the magnetosphere to external influence is ambiguous. The most vivid expression of such a response is a geomagnetic storm, during which a global restructuring of the magnetosphere occurs. One of the main manifestations of a geomagnetic storm is the magnetic field depression, which is measured at the Earth's surface at middle and low latitudes. The depression of the horizontal component of the magnetic field at the Earth's surface is caused by the development of magnetospheric current systems: magnetopause currents, ring currents, magnetospheric tail currents, and longitudinal currents. During a magnetic storm, the main contribution to the variation of the geomagnetic field in the inner regions of the magnetosphere is made by the magnetospheric tail currents and the ring current (e.g., [Kalegaev et al., 1998]). The ratio between the contributions of these current systems depends on the storm power [Kalegaev and Makarenkov, 2008; Kalegaev and Vlasova, 2017]. The non-synchronous development of these large-scale currents determines the dynamics of the magnetospheric magnetic field [Alexeev et al., 1996]. At the same time, changes in the magnetic field affect the overall structure of the magnetosphere, as well as the populations of charged particles, their position in space, and the intensity of the currents.

An example of localization of such populations are radiation belts (RBs). The Earth's radiation belts were discovered during the first space experiments more than half a century ago: the inner one by the artificial satellite Explorer-1 (James Van Allen's group) and the outer one (Sputnik-2) by the team of the Moscow State University Research Institute for Nuclear Physics under the leadership of S.N. Vernov [Vernov et al., 1960]. Unlike the inner belt, the Earth's outer electron radiation belt (EBRB) is one of the most dynamic objects of the magnetosphere. Its presence is an important factor of space weather.

The most significant variations of the Earth's outer electron radiation belt are observed during geomagnetic storms, so it is natural to expect that the geomagnetic field should be one of the main factors controlling the dynamics of electron fluxes in this region of the magnetosphere. At present, there is no universally accepted view on the sources of the dynamics of the outer electron radiation belt (e.g., the review [Baker et al., 2018] and references therein). One of the key questions is the role of adiabatic effects. At relatively slow changes in the magnetospheric magnetic field, variations of the outer radiation belt occur while adiabatic invariants are preserved. In this case, satellites register changes in the electron fluxes, which are not related to real losses or to the real arrival of new particles in the inner magnetosphere. In [McIlwain, 1966], a mechanism leading to a drop in the flux of PSD electrons during the main phase of a geomagnetic storm was first proposed - the so-called *Dst-effect* associated with

the transition of electrons from the core of the PSD to the distant *L-shells* and their subsequent return under the influence of adiabatic changes in the magnetosphere.

On the other hand, the magnetospheric processes leading to real changes in the populations of trapped electrons are obviously present. Among them: radial diffusion under the influence of unsteady electric fields [Shprits et al, 2008]; particle ejections and acceleration at interaction with waves [Horne and Thorne, 1998, Horne et al, 2005]; electron losses at magnetopause displacements under the influence of solar wind pressure pulses [Bortnik et al. 2006]; radial diffusion on magnetic field pulses [Tversky, 1968, 2004; Hudson et al, 2000], and fast substorm injections [Lazutin, 2013]. Within the framework of the theory of particle drift in electric and magnetic fields, a mechanism of "shock" injection of particles under the influence of a bipolar sudden pulse of the geomagnetic field has been proposed [Pavlov et al., 1993]. Pitch-angle particle scattering, rapid magnetopause motions under the influence of solar wind (SW) pressure pulses, lead to irreversible electron losses, which are compensated by the arrival of new particles accelerated by substorm processes and wave-particle interactions [Baker et al., 2018].

The influence of external factors on the dynamics of electron fluxes is the most important aspect of research. The results of a statistical study of the outer electron belt dynamics from Van Allen Probes (VAP) satellite data using the epoch superposition method indicate the most important conditions for electron flux growth: a long southern orientation of the interplanetary magnetic field (IMF), high solar wind speed and pressure [Li et al., 2015]. In the work of Turner et al. [2019], based on a study of 110 storms using Van Allen Probes satellite data, it is shown that a drop in the level of relativistic electrons in the outer PSD during the main phase of the storm is followed by an unpredictable amplitude replenishment during the recovery phase.

A discussion of the coordinated dynamics of the ring current and relativistic electrons of the Earth's outer radiation belt, in particular, during the recovery phase of geomagnetic storms can be found in [Tverskaya, 1986; Tverskaya, 1997]. In [Tverskaya, 1997] the results of calculation of the structure of the ring current during a geomagnetic storm are presented and it is shown that at the largest value $|Dst_{max}|$ the maximum pressure of the ring current plasma should be expected in the region where the maximum of the belt of relativistic electrons injected during magnetic storms ($L_{max)}$ is located. Thus, the dependence of the position of the maximum of the belt of relativistic electrons injected during magnetic storms (L_{max}) on the amplitude of the magnetic storm was theoretically justified:

$$|Dst_{max}| = 2.75 \cdot 10^4 \cdot L^{-4}_{max}$$

The dependence was obtained in [Tverskaya, 1986].empirically, using data from low-orbit polar satellites.

The magnetic storms of 17-18.03.2015 and 22-23.06.2015 were among the most powerful in the 24th solar activity cycle. They provided rich material on the dynamics of the outer radiation belt. In [Li et al., 2016] and [Baker et al., 2016b], the processes of acceleration and electron transport in the first and second storms, respectively, were analyzed. In [Nazarkov et al., 2018], a study of the ring current dynamics during the geomagnetic storms of 17-18.03.2015 and 22-23.06.2015 was performed. It was shown that the main contribution to the development of the ring current was made by proton fluxes with energies of ~10÷50 keV. In [Baker et al., 2016a], the results of a comparative analysis of the two storms of 2015 are presented. It is concluded that powerful substorms occurring during the development of a strong ring current during geomagnetic storms caused by coronal mass ejections play a central role in the strengthening of radiation belts.

The aim of the present work is to obtain evidence of the coordinated dynamics of magnetospheric currents and fluxes of charged particles of different nature in the Earth's magnetosphere during two geomagnetic storms on 17-18.03.2015 and 22-23.06.2015 on the basis of a comparative analysis of experimental data of simultaneous measurements of the fluxes of ring current protons and relativistic electrons of the outer radiation belt, as well as, the magnetospheric magnetic field.

2. EXPERIMENTAL DATA

This work utilizes experimental data obtained from the Van Allen Probes spacecraft (spacecraft), the first name of the mission is *Radiation Belt Storm Probes (RBSP*), (http://vanallenprobes.jhuapl.edu). The satellites investigated the core of the Earth's radiation belts [Mauk et al., 2013]. Two identical VAP satellites (A and B) are in a highly elliptical orbit: inclination -10°; orbital period - 9 hours; apogee ~6 R_E; perigee ~600-700 km. In March 2015, the orbit of the VAP spacecraft was in the evening-night sector of the magnetosphere, and in June 2015. - in the evening sector (Fig. 1). The rotation axis of the VAP spacecraft is stabilized and directed to the Sun.

Fig. 1.

In the presented work, we used angle-averaged data from the HOPE (*Helium Oxygen Proton Electron*) and REPT (*The Relativistic Electron Proton Telescope*) instruments, which are part of the ECT (*Energetic Particle, Composition, and Thermal Plasma Suite*) [Spence, et al. 2013], as well as magnetic field measurements on the EMFISIS (*Electric and Magnetic*

Field Instrument Suite and Integrated Science) instrument [Kletzing et al., 2013]. Data on the fluxes of electrons with energies of 2.1 MeV and protons with E = 51 keV were used.

To study the impact of the interplanetary medium on the Earth's magnetosphere, we used experimental data on the parameters of the solar wind and interplanetary magnetic field obtained from the ACE spacecraft located at the *L1* libration point at a distance of 1.5 million km from the Earth to the Sun (www.srl.caltech.edu/ACE/ASC/). The geomagnetic activity of the Earth's magnetosphere was characterized by the Dst *variation* (http://wdc.kugi.kyoto-u.ac.jp/). The *geomagnetic* field was modeled using the IGRF model: *International Geomagnetic Reference Field* (IGRF - *International Geomagnetic Reference* Field) - an international model or series of models of the Earth's average global magnetic field, taking into account its secular variation (https://www.ngdc.noaa.gov/IAGA/vmod/igrf.html). The variations of the magnetospheric magnetic field were reconstructed by subtracting the IGRF geomagnetic field components from the measurement data.

3. EXPERIMENTAL RESULTS

The two considered geomagnetic storms: 17-18.03.2015 with $|Dst_{max}|$ ~228 nTl and 22-23.06.2015 with $|Dst_{max}|$ ~ 195 nTl are comparable in power, but differ significantly in the conditions in the interplanetary medium in which the storms developed (Fig. 2): during 17-18.03.2015. - the NE pressure gradually increases to ~15 nPa and the storm develops predominantly at the southern orientation of the IMF; during 22-23.06.2015. - the NE pressure increases to ~25 nPa with a very sharp profile and the MMP has predominantly northern orientation during the main phase of the storm.

Fig. 2.

Spatial and temporal profiles of the fluxes of electrons with energies of 2.1 MeV, protons with E~50 keV, and the magnetospheric magnetic field are plotted for the two magnetic storms to trace the dynamics of particle fluxes and the magnetospheric magnetic field. The profiles are divided along the half-orbits between apogee and perigee into descending and ascending satellite trajectories (Fig. 3). To describe the dynamics of the trapped particle fluxes, profiles from only one satellite are given for each storm. For the first storm, measurements from the VAP-B satellite were used, and for the second storm, VAP-B was used because it best represents the dynamic processes of the GRPP. In the figure, for each profile, the arrow shows the direction of spacecraft motion.

Fig. 3.

3.1. Geomagnetic storm 17-18.03.2015.

The geomagnetic storm of 17-18.03.2015 developed after the arrival to the Earth of an interplanetary structure characterized by an increase in the solar wind pressure and under the conditions of predominantly southern orientation of the interplanetary magnetic field (left panels of Fig. 2).

It can be seen that the arrival of the shock wave (second profiles on the left panels of Fig. 3) caused variations in the profile of the electron fluxes and a small increase in the proton flux, i.e., the formation of a partial ring current, on the outer *L-shells*. The gradual development of the CT at the beginning of the main phase of the storm (the third and fourth profiles of Fig. 3) is accompanied by a significant decrease in the maximum electron flux, as well as by a shift of the outer boundary of the belt toward the Earth. It should be noted that the outer boundary of the CT and the electron belt completely coincide at the *L-shells* between 3.2 and 3.5 R_E. Under the conditions of the southern direction of the MMP, the development of the geomagnetic storm continues, the CT displacement inside the magnetosphere up to ~2 $R_E$is observed (fifth profile of Fig. 3) and the *Bz-component of* the magnetic field further increases. One should expect that at this stage the annular current becomes more symmetric, since the displacement toward the Earth of the inner boundary of the annular current has stopped (fifth and sixth profiles in Fig. 3), and the period of circulation of protons with energy ~50 keV at L ~ 3 is of the order of 4 hours, which is less than the time of development of the main phase of the storm.

At the end of the main phase of the storm (sixth profile in Fig. 3), the magnetic field structure is preserved only on the inner *L-shells (*$L < 4$), while in the outer regions the magnetic field is restored, and as a result, an increase in electron fluxes is observed.

3.2. Geomagnetic storm 22-23.06.2015.

The magnetic storm 22-23.06.2015 was preceded by a small increase in the solar wind pressure ~ 6 UT 22.06.2015 at a weak negative *Bz-component of* the MMP (Fig. 2), which caused a weak depression of the magnetic field at the Earth's surface and a slight increase in the proton fluxes of the ring current at the outer *L-shells* (Fig. 3). But the main development of the strong storm was caused by a powerful (~25 nPa) NE pressure pulse (at ~18:40 UT 22.06) and a short-term (~1 hour) southern orientation of the MMP, after which the *Bz-component of the* MMP was positive for ~5 hours (right panels of Fig. 2). Under the conditions of the northern orientation of the MMP, the NE pressure pulse can lead to the formation of a storm ring current, due to the non-adiabatic transfer of ring current particles to lower *L-shells*, and thus to the development of a geomagnetic storm [Kalegaev et al. 2015].

In profiles 2 in the right panels of Fig. 3, one can see that an increase in the proton flux is observed at the outer *L-shells*, which can be related to the enhancement of magnetospheric convection and the formation of a weak ring current. At the same time at the same *L-shells*, the electron flux slightly decreases.

The arrival of a powerful NE pressure pulse at ~18:40 UT on 22.06.2015 with a short-lived but significant negative *Bz-component of* the MMP displaced the captured protons from the outer *L-shells* inside the magnetosphere, which led to the strengthening of the ring current. After the solar wind shock, a powerful symmetric ring current immediately appears (third profiles in Fig. 3), which reaches its maximum values at this stage. The response of the electron population VRPZ becomes a decrease of the currents by an order of magnitude. Five hours later, the next profile (the fourth) shows a drop in electron fluxes by another two orders of magnitude. Such abrupt dynamics of all investigated parameters significantly differs from the observed gradual change during the storm of 17-18.03.2015 (left panels of Fig. 3).

The next profile during the maximum development of the storm (fifth profiles in Fig. 3) shows that the state has stabilized - the ring current is practically unchanged, similar to the electron fluxes.

At the initial phase of the storm recovery (fifth profiles in Fig. 3), the *Bz-component of* the magnetic field decreases by several tens of nTL despite the practically unchanged ring current, and the electron fluxes have fully recovered in intensity, with the maximum of the fluxes shifted one Earth radius inside the magnetosphere.

4. DISCUSSION

Variations in the solar wind and interplanetary magnetic field parameters directly or indirectly control the structure and dynamics of the magnetosphere, the development of magnetospheric current systems, and the transport, loss, and acceleration of charged particles. The existence of radiation belts is due to the presence of the Earth's magnetic field, which holds charged particles. In turn, the particle flows themselves create electric currents that contribute to the dynamics of the magnetospheric magnetic field. The main large-scale current systems in the magnetosphere are: magnetopause currents, tail currents, ring currents, and longitudinal currents (e.g., [Alexeev et al., 1996; 2001]). The field depression during geomagnetic perturbations is determined predominantly by the magnetospheric tail currents and the ring current (e.g., [Alexeev et al., 1996; Kalegaev et al., 1998]). In the core of the outer radiation belt, the ring current makes a determining contribution to the variation of the magnetic field. The different impact of the interplanetary medium on the magnetosphere during the two studied

storms also caused its different response, which can be seen in Fig. 2 by the dynamics of the geomagnetic indices: *Dst* and *AL*. During the entire main phase of the storm on 17.03.2015, one can observe a powerful substorm activity and strong magnetic field asymmetry. During the storm of 22-23.06.2015, the substorm activity and field asymmetry are observed predominantly during the sudden onset and at the very beginning of the main phase of the storm, actually during the impact of the pressure pulse of the solar wind (Fig. 2). The complex dynamics of the magnetospheric magnetic field, as well as, different conditions for the conservation of adiabatic variations, became the source of variations of the fluxes of both protons and electrons in the region of the outer electron radiation belt.

During the geomagnetic storm of 17-18.03.2015, the flux of protons with the energy of 51 keV in the region of the external electron radiation was smaller than during the storm of 22-23.06.2015, while the modulus of the measured value of *the Bz-component of* the interplanetary magnetic field is larger (Fig. 3). Two factors may be the reasons for the observed effect. First, different mechanisms for the formation of the main flux of the ring current during the two storms (rapid injection due to a strong solar wind pressure pulse on 22.06.2015 and successive injections during the main phase of the storm on 17.03.2015) could have formed a different energy spectrum of the ring current protons, and in this work only one population of protons with an energy of 51 keV is investigated. Second, an important factor is the difference in the contribution of the magnetospheric tail currents and the partial ring current in the locally different parts of the satellite orbits during the two storms. A detailed analysis of the observed effect is the subject of future work.

Fig. 4.

In order to reveal the global dynamics of the outer radiation belt, the time profiles of the maximum maximum current during the two storms are shown in Fig. 4 shows the time profiles of the maximum fluxes of the external RP electrons and CT protons (*a*, *b*) and their corresponding spatial location (*c*, *d*). To increase the statistics, the profiles are plotted using data from two satellites: VAP-A and VAP-B. The data are given for five days, not only during the main phases of storms, as in Fig. 3, but also during the periods of the recovery phases, as well as, one and a half days before the onset of the storm.

A few hours before the solar wind shock on 22.06.2015, the first increases of proton fluxes on the outer drift envelopes are observed, caused by the intensification of magnetospheric convection at the southern direction of the MMP (Fig. 2). The formation of a weak ring current led to a decrease of the electron fluxes at the outer *L-shells* (Fig. 3). In Fig. 4 marks the time of primary proton injection. In the main phase of the two storms, the dynamics

of the electron fluxes differ significantly as a result of different mechanisms of ring current formation. It can be seen that for the storm of 22.06.2015, the drop of the maximum electron fluxes and the change of their position are more intense than in the storm of 17.03.2015, which is consistent with the ring current dynamics.

During the recovery phase of the storms, the dynamics of the electron fluxes and all related parameters presented in Fig. 4, are very close in both cases. One can say that the development of both storms follows the same path, which is dictated by similar external conditions (Fig. 2) and the state of the magnetosphere itself. As a result of the storm, the *L-positions* of the electron flux maxima shifted one Earth radius inside the magnetosphere. The maxima began to be located at $L \sim 3.5$, which agrees well with the empirical dependence on $|Dst_{max}|$ [Tverskaya, 1986]. Such a shift can be explained by the energetic favorability of such a position of the radiation belt in the presence of a powerful ring current.

Irrespective of the storm phase, physical mechanisms related to variations of magnetic and electric fields act in the magnetosphere, which force electrons to move inside the RP: radial diffusion under the influence of unsteady electric fields and drift in crossed magnetic and electric fields. In this case, the key external factor is the solar wind electric field ($-B_zV_{sw}$), which is proportional to the electric field in the tail of the magnetosphere. As positive values of ($-B_zV_{sw}$) increase, the drift velocity of particles in crossed fields (electric and magnetic) toward Earth on the night side of the magnetosphere increases. It is this coupling function, rather than the individual parameters - B_z and V_{sw}, that is an important geoeffective parameter responsible for the development of the ring current and for the dynamics of radiation belts [Newell et al., 2007]. It was observed in [Georgiou et al., 2018] that the solar wind electric field controls the radial diffusion of particles of the Earth's radiation belts under the influence of ULF waves. This mechanism may contribute to the efficient movement of electrons deep into the radiation belts during a long period of stable morning-to-evening electric field orientation in the nighttime magnetosphere. During the main phase of the storm, the strong *Dst effect* forces electrons to move outward of the WP, so a clear correlation of the ring current dynamics and electron fluxes can be observed. At the end of the main phase, the power of *the Dst-effect* weakens, and only the result of the combined action of all mechanisms can be observed. In the recovery phase, along with radial diffusion, the reverse *Dst-effect*, i.e., the return, capture, and possible betatron acceleration of particles during the dipolarization of the geomagnetic field, begins to act along with radial diffusion [Tversky, 1968; 2004]. Radial and local electron acceleration mechanisms also operate during the recovery phase of the storm [Reeves et al., 2013], including particle injection under the influence of substorm activity and through

interaction with waves [Baker et al., 2018]. Since the power of the *Dst effect* is obviously determined by the magnitude of the variation of the magnetic field, which depends on the magnitude of the ring current, one should expect coordinated dynamics of the fluxes of trapped protons and VRPZ electrons. The results obtained in [Vlasova & Kalegaev, 2024] investigating the dynamics of the external electron radiation belt in the geostationary orbit region for a sufficiently long time (16.10.2016-16.02.2017) indicate that changes in the components of the magnetospheric magnetic field and in the electron fluxes are components of a single process occurring simultaneously with changes in the magnetosphere as a single whole. The studies carried out in the presented work indicate the coordinated dynamics of the CT proton and GRPZ electron populations during the two magnetic storms.

5. CONCLUSION

The variations of the fluxes of ring current protons and relativistic electrons of the Earth's external radiation belt according to the experimental data from the Van Allen Probes spacecraft during two geomagnetic storms of close power ($|Dst_{max}|$ ~200 nTL) on 17-18.03.2015 and 22-23.06.2015 are considered. The storm of 17-18.03.2015 developed at the southern direction of the IMF. The peculiarities of the storm development on 22-23.06.2015 are connected with a prolonged period of the northern IMF and an extremely strong pulse of solar wind pressure, which contributed to the development of the ring current.

The temporal development of the spatial profiles of the fluxes of low-energy protons with energies ~50 keV in different sectors of the magnetosphere showed two different mechanisms of the ring current formation: due to substorm injections leading to the gradual formation of the ring current and due to the magnetospheric compression under the action of the extreme solar wind pressure pulse. At the same time, similar *Dst* profiles are observed during the development of storms.

The results of the comparison of simultaneous measurements of proton and electron fluxes and the geomagnetic field indicate the coordinated dynamics of the ring current and the Earth's external radiation belt. The ring current becomes a source of the magnetic field, which leads to adiabatic decreases of electron fluxes by several orders of magnitude. During the formation of a symmetric CT and its gradual decay in the recovery phase, the state of the magnetosphere stabilizes and the electron fluxes are restored. Along with this, there are undoubtedly processes leading to real losses and replenishment of the outer electron radiation belt with new particles, but they occur against the background of global changes in the outer

radiation belt associated with the development of large-scale storm current systems leading to changes in the structure of the magnetosphere.

ACKNOWLEDGEMENTS

The authors express their sincere gratitude to the developers of the HOPE, REPT, and EMFISIS instruments for the Van Allen Probes satellites and to the CDAWEB catalog developers for providing the VAP satellite measurement data.

FUNDING

This work was supported by the Russian Foundation for Basic Research, project No. 22-62-00048.

REFERENCES

1. *Vlasova N.A., Kalegaev V.V.* On the coordinated dynamics of the magnetic field and fluxes of relativistic electrons in the geostationary orbit // Space Research. V. 62. No. 4. P. 350-361. 2024. https://doi.org/10.31857/S0023420624040058

2. *Kalegaev V.V., Alekseev I.I., Felshtein Ya.I., Gromova L.I., Grafe A., Grispan M.* Magnetic flux through lobes of the magnetosphere tail and dynamics of Dst variations // Geomagnetism and aeronomy. V. 38. P. 10-16. 1998.

3. *Kalegaev V.V., Vlasova N.A.* Relative dynamics of the ring current – magnetospheric tail currents during geomagnetic storms of varying intensity // Geomagnetism and aeronomy. V. 57. No. 5. P. 572-577. 2017. https://doi.org/10.7868/S0016794017040083

4. *Kalegaev V.V., Vlasova N.A., Peng J.* The dynamics of the magnetosphere during geomagnetic storms on 21-22.01.2005 and 14-15.XII.2006 // Space Research, V. 53, No. 2, P. 105-117. 2015. https://doi.org/10.7868/S002342061502003X

5. *Lazutin L.L.* Injection of relativistic electrons into the inner magnetosphere during magnetic storms: connection with substorms // Geomagnetism and aeronomy. V. 53 P. 10-1134. 2013.

6. *Nazarkov I.S., Kalegaev V.V., Vlasova N.A., Beresneva E.A., Bobrovnikov S.Yu., Prost A*. Dynamics of the magnetospheric magnetic field during powerful magnetic storms in 2015 according to measurements of the Van Allen Probes spacecraft and simulation results // Space Research. V. 56. No. 6. P. 41-45. 2018. https://doi.org/10.31857/S002342060002489-5

7. *Pavlov N.N., Tverskaya L.V., Tverskaya B.A., Chuchkov E.A.* Variations of energetic particles of radiation belts during a strong magnetic storm on March 24-26, 1991 // Geomagnetism and Aeronomy. V. 33. No. 6. P. 41-45. 1993.
8. *Tverskaya L.V.* On the boundary of electron injection into the Earth's magnetosphere // Geomagnetism and aeronomy. V. 26. P. 864-865. 1986.
9. *Tverskoy B.A.* Dynamics of the Earth's radiation belts. Moscow: Nauka, 224 p. 1968. (Fundamentals of Theoretical Cosmophysics. Selected works. Moscow: URSS. 336 p. 2004.)
10. *Tverskoy B.A.* The mechanism of formation of the structure of the ring current of magnetic storms // Geomagnetism and aeronomy. V. 37. № 5. P. 29-34. 1997.
11. *Alexeev I.I., Belenkaya E.S., Kalegaev V.V., Feldstein Y. I., Grafe A.* Magnetic storms and magnetotail currents // J. Geophys. Res. V. 101. № A4. P. 7737–7747. 1996. https://doi.org/10.1029/95JA03509
12. *Alexeev I.I., Kalegaev V.V., Belenkaya E.S.* The model description of magnetospheric magnetic field in the course of magnetic storm on January 9–12, 1997 // J. Geophys. Res. V. 106. № A11. P. 25683–25694. 2001.
13. *Baker D.N., Jaynes A.N., Kanekal S.G., et al.* Highly relativistic radiation belt electron acceleration, transport, and loss: Large solar storm events of March and June 2015 // J. Geophys. Res.-Space. V. 121. P. 6647–6660. 2016a. https://doi.org/10.1002/2016JA022502
14. *Baker D. N., Jaynes A. N., Turner D. L., et al.* A telescopic and microscopic examination of acceleration in the June 2015 geomagnetic storm: Magnetospheric Multiscale and Van Allen Probes study of substorm particle injection // Geophys. Res. Lett. V. 43. P. 6051–6059. 2016b. https://doi.org/10.1002/2016GL069643
15. *Baker D.N., Erickson P.J., Fennell J.F., Foster J.C., Jaynes A.N., Verronen P.T.* Space weather effects in the Earth's radiation belts // Space Sci. Rev. V. 214. № 17. P. 1–60. 2018. https://doi.org/10.1007/s11214-017-0452-7
16. *Bortnik, J., Thorne R. M., O'Brien T. P., J. C. Green J.C., Strangeway R. J., Shprits Y. Y., D. N. Baker D.N.* Observation of two distinct, rapid loss mechanisms during the 20 November 2003 radiation belt dropout event. // J. Geophys. Res. V. 111. A12216. 2006. https://doi.org/10.1029/2006JA011802
17. *Georgiou M., Daglis I.A., Rae I.J., Zesta E., Sibeck D.G., Mann I.R., Balasis G., Tsinganos K.* Ultra-low frequency waves as an intermediary for solar wind energy input into

the radiation belts. // J. Geophys. Res.-Space. V. 123. P. 10090–10108. 2018. https://doi.org/10.1029/2018JA025355
18. *Horne, R.B., and Thorne R.M.* Potential waves for relativistic electron scattering and stochastic acceleration during magnetic storms // Geophys. Res. Lett. V. 25. № 15. P. 3011–3014. 1998. https://doi.org/10.1029/98GL01002
19. *Horne, R.B., Thorne R.M., Glauert S.A., Albert J.M., Meredith N.P., Anderson R.R.* Timescale for radiation belt electron acceleration by whistler mode chorus waves. // J. Geophys. Res. V. 110. A03225. 2005. https://doi.org/10.1029/2004JA010811
20. *Hudson, M.K., Elkington S.R., Lyon J.G., Goodrich*. C.C. Increase in relativistic electron flux in the inner magnetosphere: ULF wave mode structure // Adv. Space Res. V. 25. P. 2327–2337. 2000. https://doi.org/10.1016/S0273-1177(99)00518-9
21. *Kalegaev V.V., Makarenkov E.V.* Relative importance of ring and tail currents to Dst under extremely disturbed conditions // J. Atmos. Solar-Terr. Phys. V. 70. P. 519–525. 2008. https://doi.org/10.1016/j.jastp.2007.08.029
22. *Kletzing C.A., Kurth W.S., Acuna M., et al.* The Electric and Magnetic Field Instrument Suite and Integrated Science (EMFISIS) on RBSP // Space Sci. Rev. V. 179. P. 127–181. 2013. https://doi.org/10.1007/s11214-013-9993-6
23. *Li W., Ma Q., Thorne R.M., et al.* Radiation belt electron acceleration during the 17 March 2015 geomagnetic storm: Observations and simulations // J. Geophys. Res.-Space. V. 121. P. 5520–5536. 2016. https://doi.org/10.1002/2016JA022400
24. *Li X., Selesnick R.S., Baker D.N., et al.* Upper limit on the inner radiation belt MeV electron intensity // J. Geophys. Res. V. 120. № 2. P. 1215–1228. 2015. https://doi.org/10.1002/2014JA020777
25. *Mauk B.H., Fox N.J., Kanekal S.G., Kessel R.L., Sibeck D.G., Ukhorskiy A.* Science objectives and rationale for the radiation belt storm probes mission // Space Sci. Rev. V. 179. P. 3–27. 2013. https://doi.org/10.1007/s11214–012-9908-y
26. *McIlwain C.E.* Ring current effects on trapped particles. // J. Geophys. Res. V. 71. P. 3623–3628. 1966.
27. *Newell P.T., Sotirelis T., Liou K., Meng C.-I., Rich F.J.* A nearly universal solar wind-magnetosphere coupling function inferred from 10 magnetospheric state variables. // J. Geophys. Res. V. 112. A01206. 2007. https://doi.org/10.1029/2006JA012015.

28. *Reeves G.D., Spence H.E., Henderson M.G., et al.* Electron acceleration in the heart of the Van Allen Radiation belts // Science. V. 341. P. 991–994. 2013. https://doi.org/10.1126/science.1237743
29. *Shprits Y.Y., Elkington S.R., Meredith N.P., Subbotin D.A.* Review of modeling of losses and sources of relativistic electrons in the outer radiation belt I: Radial transport // J. Atmos. Solar-Terr. Phys. V. 70. № 14. P. 1679–1693. 2008. https://doi.org/10.1016/j.jastp.2008.06.014
30. *Spence H.E., Reeves G.D., Baker D.N., et al.* Science goals and overview of the energetic particle, composition, and thermal plasma (ECT) suite on NASA's radiation belt storm probes (RBSP) mission // Space Sci. Rev. P. 311–336. 2013. https://doi.org/10.1007/s11214-013-0007-5
31. *Turner D.L., Kilpua E.K.J., Hietala H., et al*. The response of Earth's electron radiation belts to geomagnetic storms: Statistics from the Van Allen Probes era including effects from different storm drivers // J. Geophys. Res.-Space. V. 124. № 2. P. 1013–1034. 2019. https://doi.org/10.1029/2018JA026066
32. *Vernov S.N., Chudakov A.E., Vakulov P.V., Logachev Y.I.* Radiation measurement during the flight of the second Soviet space rocket // Proc. First International Space Science Symposium (Space Research). Amsterdam: North-Holland. P. 845–851. 1960.

FIGURE CAPTIONS

Fig. 1. Orbits of VAP spacecraft during two magnetic storms on 17-18.03.2015 and 22-23.06.2015.

Fig. 2. Time profiles of (*a*) solar wind velocity and (*b*) solar wind density, (*c*) *Bz-component of the* MMP, (*d*) *AL-index*, and (*e*) *Dst-index* for two magnetic storms on 17.03.2015 (left panels) and 22.06.2015 (right panels). Dark bars indicate the time intervals of the flyby of the VAP-B (left panels) and VAP-A (right panels) satellites, for which the experimental spatial and temporal profiles of the particle fluxes are given. The "left" arrows characterize the passes on descending trajectories, and the "right" arrows characterize the passes on ascending trajectories.

Fig. 3. Spatial and temporal profiles of the fluxes of electrons with E = 2.1 MeV (upper panels), protons with E = 51 keV (middle), and variations of the *Bz component of* the magnetospheric magnetic field (bottom) during the main storm phase for two magnetic storms on 17-18.03.2015 (left, from VAP-B satellite data) and 22-23.06.2015 (right, from VAP-A satellite data) between 2 and 5.8 R_E.

Fig. 4. Time profiles of the maximum fluxes at each half-orbit from data of two satellites VAP-A and VAP-B and their approximation for (*a*) electrons with E = 2.1 MeV, (*b*) protons with E= 51.8 keV; (*c*) and (*d*) *L-positions* of the maximum electron and proton fluxes, respectively; (*e*) *Dst-index* and (*f*) *Bz-component of* the MMP. The left and right panels correspond to the storms of 17.03.2015 and 22.06.2015, respectively. The time range for both storms is 4 days each. The dashed vertical straight line corresponds to the primary proton injection before the start of the storm. The dashed vertical straight lines correspond to the beginning of the geomagnetic storm.

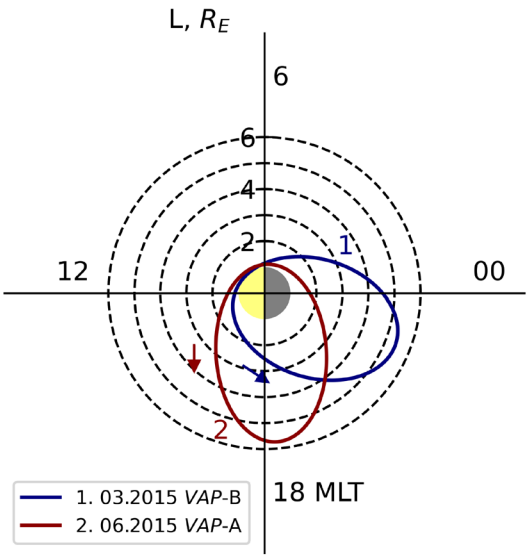

Fig. 1.

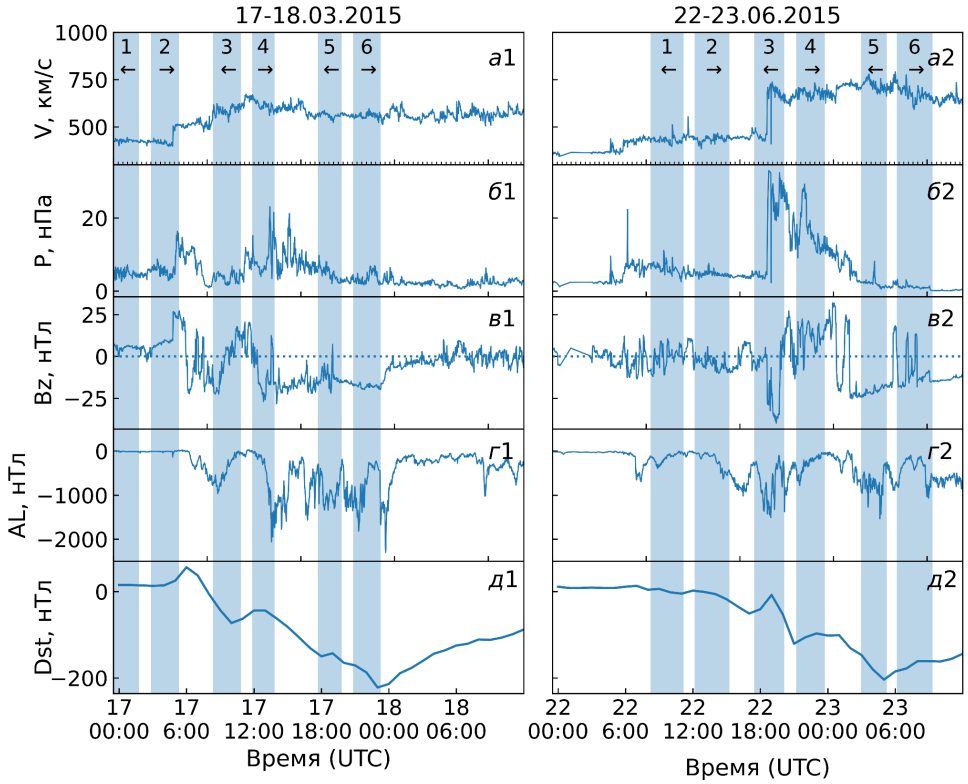
17-18.03.2015
22-23.06.2015
V, км/с
P, нПа
Bz, нТл
AL, нТл
Dst, нТл
а1
б1
в1
г1
д1
а2
б2
в2
г2
д2
Время (UTC)
Время (UTC)

Fig. 2.

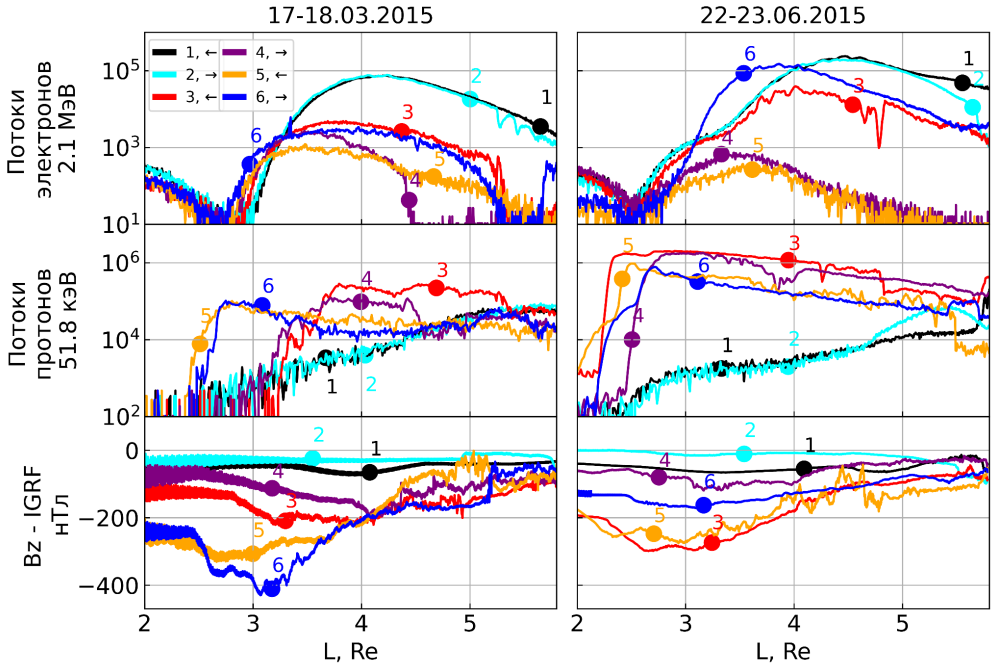
17-18.03.2015
22-23.06.2015
Потоки электронов 2.1 МэВ
Потоки протонов 51.8 кэВ
Bz - IGRF нТл
1, ←
2, →
3, ←
4, →
5, ←
6, →
L, Re
L, Re

Fig. 3.

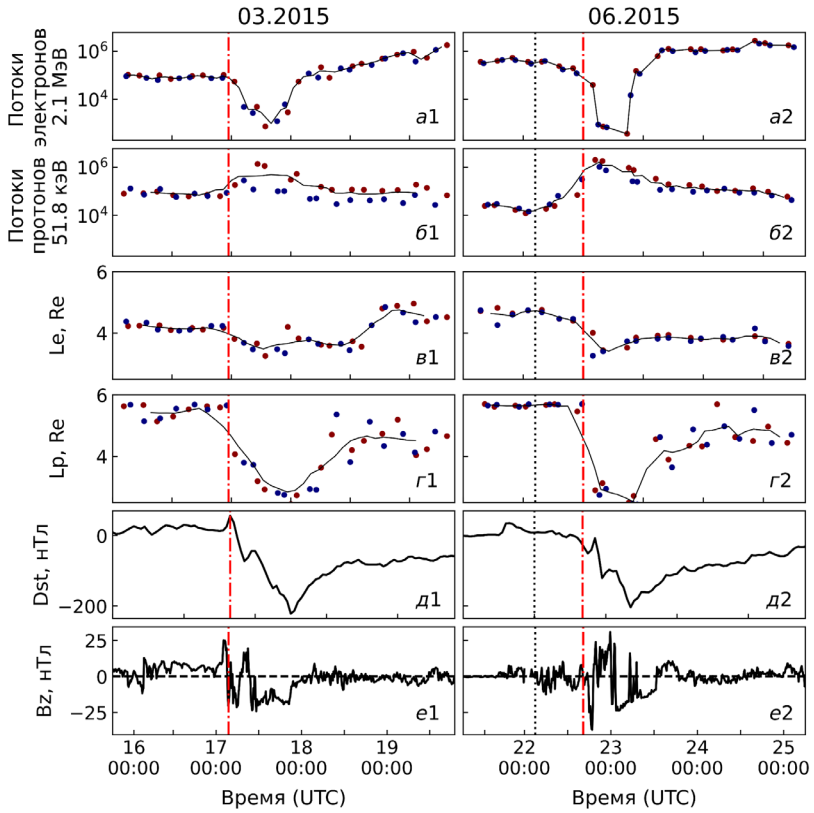
03.2015
06.2015
Потоки электронов 2.1 МэВ
Потоки протонов 51.8 кэВ
Le, Re
Lp, Re
Dst, нТл
Bz, нТл
а1
а2
б1
б2
в1
в2
г1
г2
д1
д2
е1
е2
16 00:00
17 00:00
18 00:00
19 00:00
22 00:00
23 00:00
24 00:00
25 00:00
Время (UTC)
Время (UTC)

Fig. 4.